The Neuroprotective Effect of l-Borneolum on Cerebral Ischemic Stroke by Regulating Dll4/Notch1 Pathway

Taiwei Dong
Chengdu University of TCM: Chengdu University of Traditional Chinese Medicine
Nian Chen (984962904@qq.com)
Chengdu University of TCM: Chengdu University of Traditional Chinese Medicine
https://orcid.org/0000-0002-5835-232X
Rong Ma
Chengdu University of Traditional Chinese Medicine Wenjiang Campus: Chengdu University of Traditional Chinese Medicine
Qian Xie
Chengdu University of TCM: Chengdu University of Traditional Chinese Medicine
Xiaoqing Guo
Chengdu University of TCM: Chengdu University of Traditional Chinese Medicine
Jian Wang
Chengdu University of TCM: Chengdu University of Traditional Chinese Medicine

Research

Keywords: l-Borneolum, cerebral ischemic stroke, Dll4/Notch1signaling pathway, permanent middle cerebral artery occlusion

Posted Date: November 11th, 2021

DOI: https://doi.org/10.21203/rs.3.rs-1042952/v1

Abstract

Aim

l-Borneolum is a monoterpene compound witch deserved from Blumea balsamifera (L.) DC, this study aimed to investigate the potential mechanism of l-borneolum on cerebral ischemic stroke (CIS) rats and provide evidence for the development of l-borneolum in CIS.

Methods

Permanent middle cerebral artery occlusion (pMCAO) model rats were applied to this study. Neurological function was assessed by modified neurological severity scores (mNSS) and Longa neurological function scoring methods. The pathological changes of cerebral tissue were evaluated by 2,3,5-triphenyltetrazolium chloride (TTC) and hematoxylin-eosin (HE) staining. Ultrastructure of blood brain barrier (BBB) was observed by transmission electron microscopy. Additionally, the expression of Notch1, Dll4, Hey1, Hes1, Hes5, VEGFA and p65 in the cortex were determined by Western blotting (WB) while expression of caspase 3 were determined by immunohistochemical method (IHC).

Results

l-Borneolum improved neurological function in a dose-dependently. l-Borneolum significantly alleviated brainstem edema and inflammation, as well as improved the ultrastructure of capillary and BBB in cortex. Moreover, 0.2 g/kg l-borneolum substantially decreased the protein expressions of Dll4, Notch1, Hes1, Hes5, and VEGFA in the cortex while decreased the level of Caspase-3 in the cortex of rats.

Conclusions

l-Borneolum could repair neurological function by regulating Dll4/Notch1 signaling pathway.

Introduction

Although recent researches have made breakthroughs in innovative treatment strategies, stroke is still one of the main causes of human death and disability worldwide[1]. A large number of epidemiological data show that stroke is still the second leading cause of deaths in the world and has the characteristics of high morbidity, high disability, high mortality, high recurrence rate, and high economic burden [2]. In China, the fatality rate of stroke has surpassed that of cardiovascular and cerebrovascular diseases and malignant tumors, becoming the first cause of death, seriously affecting the quality of life of patients, and bringing a heavy burden to families and society[3]. It is a common disease that seriously affects human health, of which ischemic stroke accounts for about 85% [4]. In recent years, a large number of researchers have conducted a lot of in-depth research on the treatment of cerebral ischemic stroke (CIS), and have also achieved many achievements. The following treatment methods, including thrombolysis[5,6], anti-platelet aggregation[5], statins[6], free radical scavengers[7], neuroprotective agents[10], cerebrovascular interventional therapy and other conventional treatment methods can improve

the clinical symptoms of stroke patients[6]. Both of the American Heart Association/American Stroke Association (AHA/ASA) [8] and European Stroke Organisation (ESO) [9] recommend that patients with CIS should be given rt-PA thrombolytic therapy within 3 h after the onset. However, thrombolysis, anticoagulation and fibrillation treatment have certain limitations, including a narrow therapeutic window, limited thrombolytic effect, more hemorrhagic complications, especially for large area of thrombosis, which restrict the further effect of the drug[10]. The current research progress suggests that a single therapy may not be ideal means for complex neurological diseases.

Modern studies have shown that borneol has a bidirectional regulatory effect on the CNS. On the one hand, it can prolong the coma caused by phenobarbitol sodium. On the other hand, it can prolong the time to fall asleep caused by phenobarbital and play a sedative effect [11]. In addition, borneol also has the effects of promoting the opening of the blood-brain barrier, resisting cerebral ischemia, and resisting myocardial ischemia [12]. *l*-Borneolum is the crystallization of fresh leaves of Blumea balsamifera (L.) DC. Previous studies have found that *l*-borneolum plays an anti-cerebral ischemic effect by regulating the Wnt/β-catenin signaling pathway. However, these studies only partially clarify that the potential mechanisms of *l*-borneolum on CIS is closely related to anti-inflammatory, anti-apoptotic and promoting angiogenesis[13], and has not studied the in-depth molecular biological mechanisms of its anti-CIS effects.

In this study, molecular docking technology, a computer-aided drug design technology, was used to predict the possible potential mechanism of *l*-borneolum on alleviating CIS rats. Based on the preliminary researches, this study focuses on the possible mechanisms of cerebral protection on the Notch signaling pathway. This signaling pathway was found by Thomas Hunt Morgan in 1917 that the mutation of this gene in *Drosophila* caused gaps in the wings, so the mutant gene was named as the Notch gene. The Notch signaling pathway is a highly conserved pathway in evolution. Whether in invertebrates or vertebrates, Notch signaling pathway plays an important role in cell proliferation and differentiation, morphogenesis, synaptic plasticity, and cell aging and apoptosis [14; 15]. Modern studies have found that the Notch signaling pathway plays an important role in the occurrence and development of various diseases, such as bone remodeling, tumors, and cardiovascular and cerebrovascular diseases. After cerebral ischemic injury, brain tissue damage will activate the Notch signaling pathway, causing a series of downstream reactions in the pathway, which play an important role in stem cell proliferation, differentiation, apoptosis, immune inflammation, angiogenesis, and neurogenesis [16]. In view of this, first and doremost, this study used molecular docking technology to predict the key target mechanism of *l*-borneolum in improving CIS rats and regulating the Notch signaling pathway. Additionally, we verified the effect of *l*-borneolum around Notch signaling pathway on permanent middle cerebral artery occlusion (pMCAO)-induced CIS *in vivo.* In conclusion, the present work highlighted the role of *l*-borneolum ameliorated brain injury in CIS rats by regulating Dll4/Notch1 signaling pathway. These results suggest that *l*-borneolum is the effective agent for the treatment of ischemic stroke（Figure1).

Materials And Methods

Materials

L-Borneolum (95% purity) is a crystal made by extraction and processing of fresh branches and leaves of *Blumea balsamifera* (L.) DC, was purchased from Luodian (Guizhou, China). Nimodipine was obtained from Yabao Pharmaceutical Group Co., Ltd (Shanxi, China). Ethyl carbamate (chemically pure) was obtained from Sinopharm Chemical Reagent Co., Ltd. (Shanghai, China). Tween 80 was purchased from Tianjin Chemical Reagent Co., Ltd. (Tianjin, China). Benzylpenicillin sodium for injection was obtained from Harbin Pharmaceutical Group Holding Co., Ltd. (Heilongjiang, China).

Drug preparation

The dose of *l*-borneolum in Chinese Pharmacopoeia (2020 edition) was 0.3 g/d (adult in 60 kg). The 10, 20 and 40 times of the clinical dose of *l*-borneolum were used as the low, medium and high dose group of *l*-borneolum and it was administrated as 0.05 g/kg, 0.1 g/kg, and 0.2 g/kg as our previous study[17]. Both nimodipine and *l*-borneolum were dissolved in 5% tween 80 solvent.

Molecular docking

The corresponding crystal structure of the protein is obtained from the protein data bank (https://www.rcsb.org/). The protein is pretreated by the *Protein Preparation Wizard* module in Schrödinger 2020 (Schrödinger, LLC, New York, NY, 2020), including add hydrogen and missing side chains, remove all water molecules, assign protonation states and partial charges through OPLS2005 force field. After *l*-borneolum were preprepared using the LigPrep (LigPrep, Schrödinger, LLC, New York, NY, 2020), the original small molecule in the protein is used as the ligand space to dock with the small molecule of *l*-borneolum. Finally, *l*-borneolum were docked into the binding site of proteins and evaluated by using the standard precision (SP) scoring function. The interaction relationship between receptor-ligand in molecular docking was visualized with Pymol 1.7.

Ethics statement

All animal procedures were performed in accordance with the Guide for the Care and Use of Laboratory. This study was performed in the Chinese Medicine Pharmacology Research Laboratory of Chengdu University of Traditional Chinese Medicine certified by the State Administration of Traditional Chinese Medicine (Approval NO: TCM-09-315).

Animal handing and experiment design

Male Sprague-Dawley rats, body weight 250-270 g, were obtained from the Chengdu Dashuo Biological Technology Co., Ltd. (Chengdu, China) (Permission No. SYXK (Chuan) 2014-124). In this study, an automatic temperature and humidity monitoring system was used to strictly control the breeding environment of rats. The temperature of the housing room was 25 ± 0.5 ℃. The humidity was 55 ± 5%. The light duration was 12 h: 12 h light-dark cycle. All animals were acclimatized for five days, and were free access to food and water before the experiment.

Rats were randomly divided into seven groups (twelve rats in each group), including control group, sham group, model group, vehicle group, nimodipine group (1.08×10^{-2} g/kg), *l*-borneolum low dose group (0.05 g/kg), *l*-borneolum medium dose group (0.1 g/kg), and *l*-borneolum high dose group (0.2 g/kg). Both the sham group and model group were given an equal volume of normal saline by gavage. The vehicle group was intragastrically administered with the same volume of 5% tween 80 solution. Rats in nimodipine and *l*-borneolum group were intragastrically administered with corresponding drugs for three consecutive days before modeling.

In this study, the pMCAO model was established after 30 minutes on the third day of prophylactic administration (Figure 2). Rats were anesthetized intraperitoneally with 20% ethyl carbamate solution and then fixed in the supine position. The left common carotid artery (CCA), external carotid artery (ECA), and internal carotid artery (ICA) of the rats were divided sequentially. Next, the fishing line was inserted 20 mm into the ICA through the beginning of the middle cerebral artery (MCA) to the proximal end of the anterior cerebral artery (ACA), and finally the CCA was ligated. At this moment, the time when cerebral ischemia occurred was recorded. Rats were injected with benzylpenicillin sodium for injection (100,000 units) intramuscularly. No treatment was performed for the control group. For the sham operation group, the neck skin of the rat was incised and the CCA, ECA and ICA were stripped, but the fishing line was not inserted, and the rest of the operation was the same as in other groups.

After the operation, the limbs of rats were hemiplegic to the right, and the right forelimb was bent to the inside when the tail was lifted. Rats were placed on the ground and turned to the right, or even to the right hemiplegia (as shown in Figure 1B below). The above-mentioned neurological deficits in rats indicated that the model was successful.

Rats with successfully prepared CIS model were given the corresponding drugs for three consecutive days. After the final administration, rats were sacrificed under 20% ethyl carbamate solution. Also, blood samples and brain tissue were collected. Brain samples were fixed in 10% neutral buffered formalin or stored at -80 ℃ for the detection of mRNA and protein expressions.

Recovery time detection

The righting reflex disappeared about 3 minutes after the rats were anaesthetized with ethyl carbamate, and the time point was recorded. After the CIS model was prepared, the righting reflex of the rats recovered, and the time point was recorded. The difference between the before and after time points is the time to wake up the rats after anesthesia.

Rectal temperature detection

The rectal temperature of rats in each group was measured 0.5 h before the first preventive administration, and then 0.5 h after each administration (a total of 8 measurements). The rectal temperature of rats in each group was measured every day. The rectal temperature difference before and

after administration (Δt), before and after modeling (Δt), and before and after drug withdrawal (Δt) were calculated, respectively.

Evaluation of neurological function score

The mNss and Longa scoring methods were used to assess the neurobehavioral scores of rats. At 96 h after the pMCAO surgical ischemia, the rats in each group were neurologically scored according to the mNss neurological score table. In addition, 96 h after pMCAO surgery ischemia and awakening, the rats in each group were again scored for neurological deficits according to the Zea Longa five-level 4-point method. The blinding method was adopted. Three people scored each rat in parallel, and the average value was taken for statistical analysis.

Cerebral infarction rate detection

Rats were anesthetized by intraperitoneal injection with 20% ethyl carbamate and then sacrificed. The cerebral tissue was quickly taken out, and the olfactory bulb, brain stem, and cerebellum were removed. The remaining tissue was cut into 2 mm serial sections and incubated at 37 ℃ for 30 min in 2% TTC solution (dissolved in physiological saline). These tissues were finally fixed in 4% paraformaldehyde solution for 24 h. The infarct area is white, and the normal area is red. The infarcted white area of each rat was carefully peeled off and weighed. Simultaneously, the total weight of the brain slice of each rat was weighed. The calculation formula of cerebral infarction rate is as follows: cerebral infarction rate = weight of infarct area/total weight of slice × 100%.

Morphological examination

HE staining was used to detect the morphological changes of rat cerebral tissue. The brainstem, cortex and hippocampal CA3 area of cerebral tissue were quickly collected and then fixed in neutral formalin. The paraffin-embedded brainstem, cortex and hippocampal CA3 area were cut into sections with an average of 5 μm. Finally, the brainstem, cortex and hippocampal CA3 area sections were deparaffinized, dehydrated and stained with hematoxylin eosin (H&E) for pathological evaluation. The pathological changes of brainstem, cortex and hippocampus CA3 area were observed under a 200 folds optical microscope.

Observation of the ultrastructure of rat brain cortex

Rats were anesthetized by intraperitoneal injection with 20% ethyl carbamate after the last administration for 24 h. The heart and great blood vessels of the rats were exposed. The syringe needle infused with physiological saline was inserted into the ascending aorta from the apex of the left heart of the rat. The left atrial appendage of the rat was incised as perfusion fluid. The blood in the liver of the rats was washed until the color becomes lighter or even white. Rats were perfused and fixed with 4% paraformaldehyde until the whole body became stiff, which was maintained for about 60 min. After the fixation was sufficient, the brain was removed by craniotomy, and the corresponding cerebral cortex on the ischemic side was removed. The surface water was absorbed by filter paper and fixed in 2.5%

glutaraldehyde solution, and stored at 4 ℃ for later use. After the rat brain cortex was fixed, dehydrated, embedded, sliced and stained, the microvessels and blood-brain barrier of the sample are photographed using Hitachi H-600 IV transmission electron microscope (8000 ×).

Protein extraction and Western blotting analysis

Total protein of cerebral tissue was extracted by RIPA buffer (Lot. No. 20180515, Solarbio, Beijing, China) supplemented with 1/100 phenylmethylsulfonyl fluoride (PMSF) (Lot. No. 20180313, Solarbio, Beijing, China). The lysate was centrifuged at 15, 000 g for 10 min at 4°C and the supernatant was collected. Protein concentration was determined with a BCA protein assay kit (Lot. No. 20180218, Solarbio, Beijing, China) in line with the manufacturer's recommendations. Protein samples were separated on sodium dodecyl sulfate (SDS)-polyacrylamide gels, and then transferred to polyvinylidene difluoride (PVDF) membranes (0.45 μm, Millipore, MA). The membranes were washed twice with TBS containing 0.1% Tween 20 (TBST) and incubated with blocking solution for 2 h at room temperature. The membranes were incubated overnight at 4 °C with the following primary antibodies: anti-Notch1 rabbit polyclonal antibody (3608s, Cell signaling technology, dilution: 1:1,000), anti-DLL-4 rabbit polyclonal antibody (NB600-892, Novous, dilution: 1:1,000), anti-VEGF-A mouse monoclonal antibody (ab1316, Abcam, dilution: 1:200), anti-Hes1 rabbit polyclonal antibody (D6P2U, Cell signaling technology, dilution: 1:1,000), anti-Hes5 rabbit polyclonal antibody (NBP2-27174, Novous, dilution: 1:100), anti-Hey1 rabbit polyclonal antibody (NBP1-82377, Novous, dilution: 1:1,000), anti-p65 rabbit polyclonal antibody (8242s, Cell signaling technology, dilution: 1:1,000), anti-β-actin polyclonal antibody (dilution: 1:5,000). The second day, blots were washed five times with TBST for 20 min and incubated with goat anti-rabbit IgG (H+L)/HRP secondary antibody (dilution:1:1,000) for 1 h at room temperature. Blots were again washed five times with TBST and then visualized using ECL Plus detection kit (Amersham, UK). Quantification of bands was carried out by densitometric analysis using Bio-Rad Quantity One. β-actin was used for an internal control to normalize the data.

Immunohistochemical staining

The expression of Caspase-3 levels in cerebral tissue was measured by immunohistochemical staining. Immunohistochemistry staining was performed as follows. The cardiac tissue was fixed with 4% paraformaldehyde and embedded in paraffin. anti-Caspase-3 rabbit polyclonal antibody (9662s, Cell signaling technology) was used. The images were photographed on Nikon Eclipse Ni-U microscope plus Imaging Software NIS-Elements 4.0 (Nikon, Japan) at 100 magnification.

Statistical analysis

SPSS statistical analysis software (version 17.0, SPSS Inc., Chicago, IL, USA) was used for one-way ANOVA analysis. Data were expressed as mean ± standard deviation ($\bar{X} \pm SD$). GraphPad Prism software (version 8.2.0) was used to visualize the results. Differences were statistically significant at $P < 0.05$ and highly significant at $P < 0.01$. Other matters related to materials and methods are showed in the figure legend.

Table 1. Docking parameters of important targets of *l*-borneolum intervention in CIS.

Protein name	Crystal name	Concordance score	No. of hydrogen bonds	Docking score (kcal/mol)
CATK	6QBS	3	1	-4.287
Hey1	3MY0	7	1	-4.683
Notch2	4HY0	3	1	-4.028
p53	5OC8	6	2	-5.947
HIF-1α	4ZQD	5	1	-6.208
Notch1	4WLZ	6	2	-3.914
STAT3	1Q1M	1	1	-4.349
p65	6NV2	1	2	-4.801
VEGFA	4QAF	7	2	-6.908

Results

Molecular docking analysis

Molecular docking approach can be performed to screen the effective substances of TCM, and predict the targets of specific drugs acting on specific diseases, as well as facilitate exploration of the mechanism of action[18]. According to the previous study, the protective and therapeutic effects of *l*-borneolum on CIS was closely related to regulate 9 important targets, including cathepsin K (CATK), Hey1, Notch-2, p53, hypoxia-inducible factor 1-alpha (HIF-1α), Notch1, signal transducer and activator of transcription 3 (STAT3), p65, and vascular endothelial growth factor A (VEGFA). The docking parameters of important targets of *l*-borneolum intervention in CIS were listed in Table 1. A total of nine sets of docking scoring data were obtained in this study. It is generally believed that the smaller the binding energy of the active components and the relevant target, the more stable binding. The nine sets of docking data showed that the docking scores of VEGFA, HIF-1α and p53were less than -5 kcal/mol (Table 1.). It indicated these three proteins had better binding ability.

According to the molecular docking results of *l*-borneolum with crucial targets of CIS, it was found that *l*-borneolum could better combined with the proteins in Notch signaling pathway (Figure 3). Notch signaling pathway is closely related to a variety of human diseases[19]. In encephalopathy, Notch1, and its key factors, Hes1 and Hes5 proteins participate in the induction of neurogenesis, angiogenesis, neural stem cell proliferation, differentiation, and cell apoptosis [20]. VEGFA and Hey1 play an important role in the repair and regeneration of blood vessels after injury. The corresponding inflammation and apoptosis regulated downstream by p65 are of great significance for the repair after ischemic brain injury. These proteins are downstream target proteins of the Notch signaling pathway [21]. Our previous studies

indicated that the molecular biological mechanism of *l*-borneolum in the treatment of CIS based on the Wnt/β-catenin signaling pathway, it also partially explored the mechanism of *l*-borneolum in improving angiogenesis, inflammation, and apoptosis after cerebral ischemic injury[13]. However, due to the complex mechanism after the onset of CIS, TCM has the characteristics of multiple levels and multiple targets. Therefore, this study was focus on the Notch signaling pathway and its downstream regulation of neurogenesis, angiogenesis, anti-apoptosis and other pathways to explore the potential mechanism of *l*-borneolum in the treatment of CIS.

Effects of *l*-borneolum on recovery time and rectal temperature of rats

Firstly, the therapeutic effect of *l*-borneolum on recovery time and rectal temperature were measured. As shown in Figure 4A, compared with the sham group, the model group, vehicle group and nimodipine group had no significant difference in the recovery time of CIS rats ($P > 0.05$). Compared with the model group, the vehicle group and nimodipine group showed no significant difference in the recovery time of CIS model rats ($P > 0.05$). However, compared with the vehicle group, the *l*-borneolum high-dose group could significantly prolong the recovery time of CIS model rats ($P < 0.01$). Although the *l*-borneolum medium- and low-dose group had a tendency to prolong the recovery time of rats, there was no significant difference ($P > 0.05$).

Rats were given the corresponding drugs prophylactically for 3 days, and therapeutically administered for 3 days after establishing an ischemic stroke model. The daily change trend of rectal temperature of rats in each group was shown in Figure 4B. The change trend of rectal temperature was analyzed, and the results indicated that the rectal temperature changes of rats were the most obvious in the three time periods, including before and after administration (1 h), before and after modeling (1 d), and before and after withdrawal (1 d). Therefore, the anal temperature difference of each group of rats at these three time points was statistically analyzed (Figure 4C-E).

Compared with the sham group, there was no significant difference in the model group and the vehicle group as for before and after administration (Δt1) ($P > 0.05$) (Figure 3C), before and after drug withdrawal (Δt3) ($P > 0.05$) (Figure 3E). However, there was substantially difference in the model group and the vehicle group as for before and after modeling (Δt2) ($P < 0.01$) (Figure 4D). Compared with the model group, the nimodipine group and the *l*-borneolum medium-dose group could substantially increased the rectal temperature of CIS rats before and after administration (Δt1) ($P < 0.05$) (Figure 3C); the *l*-borneolum high-dose group could markedly decrease the rectal temperature of CIS rats before and after modeling (Δt2) ($P < 0.05$) (Figure 4D). Nevertheless, compared with the model group and the vehicle group, there was no significant difference in each dose group of *l*-borneolum of CIS rats before and after drug withdrawal (Δt3) ($P > 0.05$) ($P > 0.05$).

Effects of *l*-borneolum on neurological function score and cerebral infarction of rats

In this study, the mNss and Longa neurological function score were used to evaluate the effect of *l*-borneolum on neurological function in CIS rats. As shown in Figure 5, compared with the sham operation

group, the mNss and Longa neurological function score of the model group and the vehicle group increased significantly ($P < 0.01$); compared with the model group, there was no significant difference in the vehicle group ($P > 0.05$), but the nimodipine group could significantly reduce the mNss and Longa neurological function scores of CIS rats ($P < 0.05$ or $P < 0.01$) (Figure 5A, B). Compared with the vehicle group, the *l*-borneolum medium- and high-dose group could dramatically reduce the mNss and Longa neurological function scores of CIS rats ($P < 0.05$ or $P < 0.01$) (Figure 5A, B). The results of mNss and Longa neurological function scores suggested that *l*-borneolum could protect the neurological function of rats with cerebral ischemia injury to varying degrees.

Next, the cerebral infarction of CIS rats was assessed. It could be seen from Figure 5D that the cerebral tissue of the sham group was rosy and no pale infarcts were formed. The cerebral tissue slices of the model group and the vehicle group had a larger area of white infarcts. The nimodipine group had smaller infarctions than the model group. The infarct size of the *l*-borneolum medium- and high-dose group was smaller than the vehicle group. The results of statistical analysis showed that compared with the sham group, the cerebral infarction rate of CIS rats in model and vehicle group increased significantly ($P < 0.01$); compared with the model group, there was no significant difference in the cerebral infarction rate of rats in the vehicle group ($P > 0.05$), while the cerebral infarction rate of rats in the nimodipine group was extremely significantly reduced ($P < 0.01$); compared with the vehicle group, the cerebral infarction rate of rats in the three dose groups of *l*-borneolum were significantly reduced ($P < 0.05$ or $P < 0.01$) (Figure 5C). The visual observation result was consistent with the statistical analysis result.

Effects of *l*-borneolum on pathological changes of cerebral tissue

The characteristic of cerebral tissue in CIS rats were no obvious abnormalities in the sham group. There was mild edema in the brain stem area and hippocampal CA3 area, which may be caused by a certain degree of inflammation in the brain stem during the ligation process of CCA and ECA and the collection of materials (Figure 6A). Compared with rats in the sham group, the cortical and hippocampal CA3 area of the model and vehicle group showed extremely significant pathological damage ($P < 0.01$) (Figure 6C, D). Compared with the vehicle group, the *l*-borneolum low-dose group significantly reduced the pathological damage of the brain stem area ($P < 0.05$) (Figure 6B). The *l*-borneolum low- and high-dose group could dramatically reduce the damage of rat cortical area ($P < 0.05$) (Figure 6C). Although the hippocampal CA3 area of each dose group of *l*-borneolum had cell necrosis, inflammation and edema, it could be clearly observed that the overall structure of hippocampal CA3 area was relatively dense with no obvious large-scale necrosis ($P > 0.05$) (Figure 6D). Overall, *l*-borneolum could alleviate the pathological damage of the brain stem, cortical and hippocampus CA3 area of CIS rats to varying degrees, especially could memorably reduce the pathological damage of cortical neurons and the formation of infarcts thereby exerting a therapeutic effect on the cerebral.

Effect of *l*-borneolum on ultrastructure of capillaries and blood-brain barrier in rats

As shown in Figure 7, in the sham group, the ultrastructure of capillaries and blood-brain barrier were well open and the surrounding tissues were normal. The basement membrane was continuous. The

mitochondrial crests of endothelial cells were clear, and the organelles were relatively complete. In the vehicle group, the capillaries and blood-brain barrier were discontinuous, and the connection with endothelial cells was loose. The tissue around the blood vessel was severely edema. The organelles in the endothelial cells disappeared. The mitochondrial cristae disappeared, and the structure was loose. The capillaries in the *l*-borneolum group had better openness, the layer of the blood vessel wall was clear, and there was mild swelling around it. The organelles in the endothelial cells were clearly visible. In addition, the intact mitochondrial cristae could be seen, and the tissue around the blood vessel was edema. Compared with rats in the vehicle group, the microvascular structure of the rats in each administration of *l*-borneolum group had been ameliorated, mainly in the improvement of endothelial cell organelles and blood vessel walls, and the tissue edema around the capillaries had also been improved to a certain extent.

Effects of *l*-borneolum on the relative protein expression of Hes5, Notch1, Hes1, Dll4, p-65, and VEGFA in rats

The Notch pathway is highly conservative in the evolutionary process. It exists at all stages from lower organisms to higher organisms, affecting cell proliferation, differentiation, synaptic plasticity, and promoting stem cell self-renewal. To further confirm that *l*-borneolum plays an important role in Notch1-related signaling pathway, the protein expression levels of Hes5, Notch1, Hes1, Dll4, p-65, and VEGFA in different groups in the cerebral cortex of CIS rats were detected by Western Blotting (Figure 8A). The results indicated that compared with the sham group, the relative protein expression of Hes5, Notch1, Hes1, Dll4, p-65, and VEGFA in the cerebral cortex of the vehicle group were dramatically upregulated ($P < 0.01$) (Figure 8B-G). Compared with the vehicle group, the *l*-borneolum high-dose group could substantially decrease the relative protein expression of Hes5, Notch1, Hes1, Dll4, p-65, and VEGFA in the cerebral cortex area of CIS rats ($P < 0.05$ or $P < 0.01$). The results suggested that the therapeutic effects of *l*-borneolum on CIS rats might be related to its inhibition of the Notch1 pathway and down-regulation of the downstream related protein expression, thereby improving cerebral ischemia injury and exerting a therapeutic effect on the cerebral.

Furthermore, immunohistochemical staining was used to detect the relative protein expression level of Caspase-3 in the cerebral cortex of the CIS rats. Compared with the sham group, the relative protein expression of Caspase-3 in the cerebral cortex area of the vehicle group increased significantly ($P < 0.01$) (Figure 8H, I). Conversely, compared with the vehicle group, the *l*-borneolum high-dose group could significantly reduce the relative protein expression optical density of Caspase-3 in the CIS rats ($P < 0.05$) (Figure 8H, I).

Discussion

CIS is primarily caused by the stenosis and occlusion of the internal vertebral and carotid arteries, and is considered as the most dangerous type of stroke[22]. Clinical thrombolytic therapy has a narrow therapeutic window and limited thrombolytic effect. For this kind of acute disease, there are certain

limitations. At present, finding the new CIS treatment scheme and agent are a trending and important topic in clinical medical research [23]. Our previous research found that *l*-borneolum has a certain brain protection effect. This study was aimed to analyze the therapeutic effect of *l*-borneolum on CIS, and analyzed the molecular biological mechanism of its therapeutic effect on cerebral ischemia injury. This study was of great significance in guiding the rational selection of drugs for clinical CIS cases, so as to provide reliable evidence for the therapeutic effects of *l*-borneolum on CIS and laid a solid foundation for follow-up research.

In the pharmacodynamic section of this study, the therapeutic effects of *l*-borneolum on recovery time, rectal temperature, neurological function score, cerebral infarction rate, pathological changes of CIS rat were explored. The results of the study found that *l*-borneolum could prolong the recovery time of pMCAO model rats in a dose-dependent manner, showing a sedative effect. Dynamic monitoring of the rectal temperature of rats found that it had a greater change tendency in the process of drug administration, modeling and treatment stage. At the time nodes before and after the modeling, the rectal temperature of the rats in the *l*-borneolum group changed the most, reflecting that *l*-borneolum could markedly reduce the rectal temperature of the CIS rats during the cerebral injury, and played a brain protection effect. After modeling, the high-dose *l*-borneolum group could substantially reduce the rectal temperature of CIS rats. However, after the drug withdrawal, although the rectal temperature of the rats in the *l*-borneolum group dropped slightly, there was no significant difference, and it basically remained above 36.5℃, maintaining the body temperature of the rats within the range of normal vital signs.

In this study, the mNss and Longa neurological function scoring methods were used to investigate the therapeutic effect of *l*-borneolum on CIS rats. The results of the study showed that the mNss and Longa neurological function scores of the rats in each group were substantially higher than those in the sham group, reflecting that the rats showed different degrees of neurological deficit or damage after modeling. At the same time, the results indicated that the CIS model was successful and stable. In the mNss and Longa neurological function score tests, *l*-borneolum could markedly reduce the neurological deficit of CIS rats. The two scoring results were basically consistent with each other, and showing a certain dose-dependent. In addition, this study explored the effect of *l*-borneolum on the cerebral infarction rate of CIS rats, and found that the cerebral infarction rate of rats in the *l*-borneolum group was significantly decreased. It showed that *l*-borneolum could alleviate and repair the tissue damage around the ischemic infarction, and reduce the apoptosis and necrosis around the ischemic penumbra in a dose-dependent way. Histopathological results showed that *l*-borneolum significantly reduced inflammation and cell edema in the brainstem area. Simultaneously, *l*-borneolum improve and repair the cellular edema of the cortex. Each administration group of *l*-borneolum could reduce the tendency of hippocampal CA3 injury. In summary, *l*-borneolum could alleviate the pathological structure of brain stem area, cortical area and hippocampus CA3 area of CIS model rats to a certain extent, but the main target is in the cortical area, which could significantly reduce the formation of cerebral infarction. These results were basically the same as the neurological function score, cerebral infarction, and lower body temperature after modeling. It was suggested that the main target of *l*-borneolum to alleviate brain tissue damage after ischemia is

concentrated on the cortex of the ischemic side. It is speculated that *l*-borneolum enters the BBB to regulate the brainstem reticular ascending system to play a therapeutic role in the cerebral.

Notch is a membrane receptor that regulates cell proliferation, differentiation and developmental fate within a certain range. During the development of the brain, the Notch signaling pathway promotes the partial maintenance of neural progenitor cells by inhibiting neurogenesis[24]. NICD is the intracellular active site of Notch. The transfer of NICD to the nucleus will cause the transcription and expression of Hes and Hey family genes, resulting a series of biological effects. Notch's receptors include Notch1, Notch2, Notch3, and Notch4, which bind to different ligands and play an important role in the growth and development of nerve cells [25; 26]. Under physiological conditions, the Notch pathway is in a resting state. After cerebral ischemia injury, the Notch signaling pathway is activated to regulate downstream p-JNK, p65, Bax and Caspase family-related proteins, thereby controlling the occurrence of the apoptotic cascade [27]. Regulating the expression of Hey family members, downstream of Notch, can promote the regeneration and repair of capillaries. In addition, studies have shown that the negative feedback regulation of VEGFA and Dll4-Notch1 signaling pathway is directly related to the reconstruction of a good vascular network [28; 29; 30]. Another important family of proteins downstream of Notch is the Hes family, of which Hes1, Hes2, Hes5 play an important role in regulating the proliferation, differentiation and neurogenesis of stem cells and vascular smooth muscle. Simultaneously, they have a synergistic effect with the angiogenesis effect of VEGF [31; 32]. Studies have also reported the possible mechanism of Notch1 and VEGFA on the activation and transformation of astrocytes into neurons [33]. In short, the Notch signaling pathway plays an important role in the repair of damage after cerebral ischemia. Based on molecular docking technology, this study found that *l*-borneolum binds well to Notch1, VEGF, p65, and Hey1 proteins. These targets are all important site proteins in the Notch signaling pathway. This study found that the relative protein expression level of Notch1, Hes5, Notch1, Hes1, Dll4, p-65, and VEGFA in the vehicle group of ischemic cortical was significantly increased. This result is consistent with previous study[34]. The relative protein expression of Notch1, Hes5, Notch1, Hes1, Dll4, p-65, and VEGFA in the ischemic cortex of the *l*-borneolum group significantly decreased. Therefore, whether it is from the therapeutic effect of *l*-borneolum on NVU, the prediction results of molecular docking, and even the verification of molecular biological mechanism, it has been found that the mechanism of *l*-borneolum in improving brain injury after CIS may be closely related to the Notch signaling pathway.

Cerebral ischemia damage exacerbates the activation of γ-secretase, causing the cleavage of the intracellular segment of Notch1 into NICD, which further activates downstream related effects. Under ischemic conditions, the enhancement of the Notch signaling pathway causes downstream neuronal apoptosis cascades[35]. In experiments with mice with Notch gene knockout, brain damage caused by ischemic stroke was rarely found[36]. After cerebral ischemia, JNK/cJun pro-apoptotic markers increase with the increase of Notch1. Overexpression of NICD can promote the activation of JNK/cJun signaling pathway and aggravate cell apoptosis[37]. All the evidence proves that inhibiting Notch1 signaling pathway can avoid neuronal apoptosis. This study showed that *l*-borneolum can inhibit the protein expression of Notch1 and reduce the downstream p65 and Caspase3 protein expression. *L*-Borneolum may inhibit Notch1-p65-Caspase3 to reduce the signal pathway of neuronal apoptosis in the cortex after

cerebral ischemia injury, thereby inhibiting neuronal apoptosis and playing a therapeutic effect on the brain (Figure 8).

Conclusion

In conclusion, the present work revealed that *l*-borneolum plays a crucial role in brain protection by regulating the Notch pathway in CIS rats. *l*-Borneolum have effect on reducing the rectal temperature of CIS rats, promoting the recovery of neurological function, reducing the rate of cerebral infarction, and alleviating the pathological damage of the brain stem, cortical, and hippocampal CA3 area tissues in a dose-dependent manner. The potential mechanism of *l*-borneolum on CIS may be related to inhibiting the Notch signaling pathway, promoting vascular network reconstruction and neurogenesis in damaged cerebral cortex, protecting brain capillary and BBB, and then stabilize and remodel NVU. The results provided a new promising therapeutic agent for prevention and treatment of CIS (Figure 9). However, further clinical trials are necessary for further confirming the conclusions.

Abbreviations

CIS, cerebral ischemic stroke; AHA/ASA, American Heart Association/American Stroke Association; ESO, European Stroke Organisation; SPRG, Stroke Progress Review Group; NVU, neurovascular unit; CNS, central nervous system; ECM, extracellular matrix; BBB, blood-brain barrier; TCM, traditional Chinese medicine; pMCAO, permanent middle cerebral artery occlusion; CCA, left common carotid artery; ECA, external carotid artery; ICA, internal carotid artery; MCA, middle cerebral artery; ACA, anterior cerebral artery; H&E, hematoxylin eosin; SDS, sodium dodecyl sulfate; PVDF, polyvinylidene difluoride; CATK, cathepsin K; HIF-1α, hypoxia-inducible factor 1-alpha; STAT3, signal transducer and activator of transcription 3; VEGFA, vascular endothelial growth factor A.

Declarations

Acknowledgements

This work was supported by grants from the National Natural Science Foundation of China (82104412 and 81873023), Natural Science Basic Research Program of Shaanxi Province (2020JQ-865) and Education Department of Shaanxi Province (20JK0597).

Conflict of interest

All authors claim that there are no conflicts of interest.

References

[1] M. Kawabori, H. Shichinohe, S. Kuroda, and K. Houkin, Clinical Trials of Stem Cell Therapy for Cerebral Ischemic Stroke. Int J Mol Sci 21 (2020).

[2] R.V. Krishnamurthi, T. Ikeda, and V.L. Feigin, Global, Regional and Country-Specific Burden of Ischaemic Stroke, Intracerebral Haemorrhage and Subarachnoid Haemorrhage: A Systematic Analysis of the Global Burden of Disease Study 2017. Neuroepidemiology 54 (2020) 171-179.

[3] G.B.D.D. Collaborators, The Burden of Dementia due to Down Syndrome, Parkinson's Disease, Stroke, and Traumatic Brain Injury: A Systematic Analysis for the Global Burden of Disease Study 2019. Neuroepidemiology (2021) 1-11.

[4] P. Tadi, and F. Lui, Acute Stroke, StatPearls, Treasure Island (FL), 2021.

[5] T.F. Cheng, J. Zhao, Q.L. Wu, H.W. Zeng, Y.T. Sun, Y.H. Zhang, R. Mi, X.P. Qi, J.T. Zou, A.J. Liu, H.Z. Jin, and W.D. Zhang, Compound Dan Zhi tablet attenuates experimental ischemic stroke via inhibiting platelet activation and thrombus formation. Phytomedicine 79 (2020) 153330.

[6] B.E. Sanz-Cuesta, and J.L. Saver, Lipid-Lowering Therapy and Hemorrhagic Stroke Risk: Comparative Meta-Analysis of Statins and PCSK9 Inhibitors. Stroke (2021) STROKEAHA121034576.

[7] Y.P. Vdovychenko, O.A. Loskutov, O.A. Halushko, M.A. Trishchynska, D.O. Dziuba, T.M. Povietkina, and A.D. Vitiuk, Acute Ischemic Stroke in Women: Efficacy of the Free Radical Scavenger Edaravone. Wiad Lek 74 (2021) 72-76.

[8] M. Abbas, D.T. Malicke, and J.T. Schramski, Stroke Anticoagulation, StatPearls, Treasure Island (FL), 2021.

[9] E. Berge, W. Whiteley, H. Audebert, G.M. De Marchis, A.C. Fonseca, C. Padiglioni, N.P. de la Ossa, D. Strbian, G. Tsivgoulis, and G. Turc, European Stroke Organisation (ESO) guidelines on intravenous thrombolysis for acute ischaemic stroke. Eur Stroke J 6 (2021) I-LXII.

[10] H. Ma, Z. Jiang, J. Xu, J. Liu, and Z.N. Guo, Targeted nano-delivery strategies for facilitating thrombolysis treatment in ischemic stroke. Drug Deliv 28 (2021) 357-371.

[11] J.Y. Chen, X.T. Huang, J.J. Wang, and Y. Chen, In vivo effect of borneol on rat hepatic CYP2B expression and activity. Chem Biol Interact 261 (2017) 96-102.

[12] Y. Li, M. Ren, J. Wang, R. Ma, H. Chen, Q. Xie, H. Li, J. Li, and J. Wang, Progress in Borneol Intervention for Ischemic Stroke: A Systematic Review. Front Pharmacol 12 (2021) 606682.

[13] T. Dong, N. Chen, X. Ma, J. Wang, J. Wen, Q. Xie, and R. Ma, The protective roles of L-borneolum, D-borneolum and synthetic borneol in cerebral ischaemia via modulation of the neurovascular unit. Biomed Pharmacother 102 (2018) 874-883.

[14] S.J. Bray, Notch signalling: a simple pathway becomes complex. Nat Rev Mol Cell Biol 7 (2006) 678-89.

[15] S.J. Bray, Notch signalling in context. Nat Rev Mol Cell Biol 17 (2016) 722-735.

[16] T.V. Arumugam, S.H. Baik, P. Balaganapathy, C.G. Sobey, M.P. Mattson, and D.G. Jo, Notch signaling and neuronal death in stroke. Prog Neurobiol 165-167 (2018) 103-116.

[17] W. Zhang, J. Wen, Y. Jiang, Q. Hu, J. Wang, S. Wei, H. Li, and X. Ma, l-Borneol ameliorates cerebral ischaemia by downregulating the mitochondrial calcium uniporter-induced apoptosis cascade in pMCAO rats. J Pharm Pharmacol 73 (2021) 272-280.

[18] X. Jiao, X. Jin, Y. Ma, Y. Yang, J. Li, L. Liang, R. Liu, and Z. Li, A comprehensive application: Molecular docking and network pharmacology for the prediction of bioactive constituents and elucidation of mechanisms of action in component-based Chinese medicine. Comput Biol Chem 90 (2021) 107402.

[19] P. Pagella, L. de Vargas Roditi, B. Stadlinger, A.E. Moor, and T.A. Mitsiadis, Notch signaling in the dynamics of perivascular stem cells and their niches. Stem Cells Transl Med (2021).

[20] Q. Gao, A. Leung, Y.H. Yang, B.W. Lau, Q. Wang, L.Y. Liao, Y.J. Xie, and C.Q. He, Extremely low frequency electromagnetic fields promote cognitive function and hippocampal neurogenesis of rats with cerebral ischemia. Neural Regen Res 16 (2021) 1252-1257.

[21] H. Muller, J. Hu, R. Popp, M.H.H. Schmidt, K. Muller-Decker, J. Mollenhauer, B. Fisslthaler, J.A. Eble, and I. Fleming, Deleted in malignant brain tumors 1 is present in the vascular extracellular matrix and promotes angiogenesis. Arterioscler Thromb Vasc Biol 32 (2012) 442-8.

[22] A.A. Rabinstein, Update on Treatment of Acute Ischemic Stroke. Continuum (Minneap Minn) 26 (2020) 268-286.

[23] C. Zhong, C. Yin, G. Niu, L. Ning, and J. Pan, MicroRNA miR-497 is closely associated with poor prognosis in patients with cerebral ischemic stroke. Bioengineered 12 (2021) 2851-2862.

[24] Z. Chen, Y. Zhu, X. Fan, Y. Liu, and Q. Feng, Decreased expression of miR-184 restrains the growth and invasion of endometrial carcinoma cells through CDC25A-dependent Notch signaling pathway. Am J Transl Res 11 (2019) 755-764.

[25] I.T. Fiddes, G.A. Lodewijk, M. Mooring, C.M. Bosworth, A.D. Ewing, G.L. Mantalas, A.M. Novak, A. van den Bout, A. Bishara, J.L. Rosenkrantz, R. Lorig-Roach, A.R. Field, M. Haeussler, L. Russo, A. Bhaduri, T.J. Nowakowski, A.A. Pollen, M.L. Dougherty, X. Nuttle, M.C. Addor, S. Zwolinski, S. Katzman, A. Kriegstein, E.E. Eichler, S.R. Salama, F.M.J. Jacobs, and D. Haussler, Human-Specific NOTCH2NL Genes Affect Notch Signaling and Cortical Neurogenesis. Cell 173 (2018) 1356-1369 e22.

[26] C.S. Nowell, and F. Radtke, Notch as a tumour suppressor. Nat Rev Cancer 17 (2017) 145-159.

[27] Z. Li, J. Wang, C. Zhao, K. Ren, Z. Xia, H. Yu, and K. Jiang, Acute Blockage of Notch Signaling by DAPT Induces Neuroprotection and Neurogenesis in the Neonatal Rat Brain After Stroke. Transl Stroke

Res 7 (2016) 132-40.

[28] G. D'Amato, G. Luxan, G. del Monte-Nieto, B. Martinez-Poveda, C. Torroja, W. Walter, M.S. Bochter, R. Benedito, S. Cole, F. Martinez, A.K. Hadjantonakis, A. Uemura, L.J. Jimenez-Borreguero, and J.L. de la Pompa, Sequential Notch activation regulates ventricular chamber development. Nat Cell Biol 18 (2016) 7-20.

[29] M. Hellström, L.K. Phng, J.J. Hofmann, E. Wallgard, L. Coultas, P. Lindblom, J. Alva, A.K. Nilsson, L. Karlsson, N. Gaiano, K. Yoon, J. Rossant, M.L. Iruela-Arispe, M. Kalén, H. Gerhardt, and C. Betsholtz, Dll4 signalling through Notch1 regulates formation of tip cells during angiogenesis. Nature 445 (2007) 776-80.

[30] G. Zhu, Y. Lin, H. Liu, D. Jiang, S. Singh, X. Li, Z. Yu, L. Fan, S. Wang, J. Rhen, W. Li, Y. Xu, J. Ge, and J. Pang, Dll4-Notch1 signaling but not VEGF-A is essential for hyperoxia induced vessel regression in retina. Biochem Biophys Res Commun 507 (2018) 400-406.

[31] Y. Xie, W. Huang, B. Zheng, S. Li, Q. Liu, Z. Chen, W. Mai, R. Fu, and D. Wu, All-in-One Porous Polymer Adsorbents with Excellent Environmental Chemosensory Responsivity, Visual Detectivity, Superfast Adsorption, and Easy Regeneration. Adv Mater 31 (2019) e1900104.

[32] T. Zhou, W. Xu, N. Zhang, Z. Du, C. Zhong, W. Yan, H. Ju, W. Chu, H. Jiang, C. Wu, and Y. Xie, Ultrathin Cobalt Oxide Layers as Electrocatalysts for High-Performance Flexible Zn-Air Batteries. Adv Mater 31 (2019) e1807468.

[33] N.J. Shah, A.S. Mao, T.Y. Shih, M.D. Kerr, A. Sharda, T.M. Raimondo, J.C. Weaver, V.D. Vrbanac, M. Deruaz, A.M. Tager, D.J. Mooney, and D.T. Scadden, An injectable bone marrow-like scaffold enhances T cell immunity after hematopoietic stem cell transplantation. Nat Biotechnol 37 (2019) 293-302.

[34] X.Z. Hao, L.K. Yin, J.Q. Tian, C.C. Li, X.Y. Feng, Z.W. Yao, M. Jiang, and Y.M. Yang, Inhibition of Notch1 Signaling at the Subacute Stage of Stroke Promotes Endogenous Neurogenesis and Motor Recovery After Stroke. Front Cell Neurosci 12 (2018) 245.

[35] M. Ma, X. Wang, X. Ding, J. Teng, F. Shao, and J. Zhang, Numb/Notch signaling plays an important role in cerebral ischemia-induced apoptosis. Neurochem Res 38 (2013) 254-61.

[36] L. Alberi, Z. Chi, S.D. Kadam, J.D. Mulholland, V.L. Dawson, N. Gaiano, and A.M. Comi, Neonatal stroke in mice causes long-term changes in neuronal Notch-2 expression that may contribute to prolonged injury. Stroke 41 (2010) S64-71.

[37] Y.L. Cheng, Y. Choi, W.L. Seow, S. Manzanero, C.G. Sobey, D.G. Jo, and T.V. Arumugam, Evidence that neuronal Notch-1 promotes JNK/c-Jun activation and cell death following ischemic stress. Brain Res 1586 (2014) 193-202.

Figures

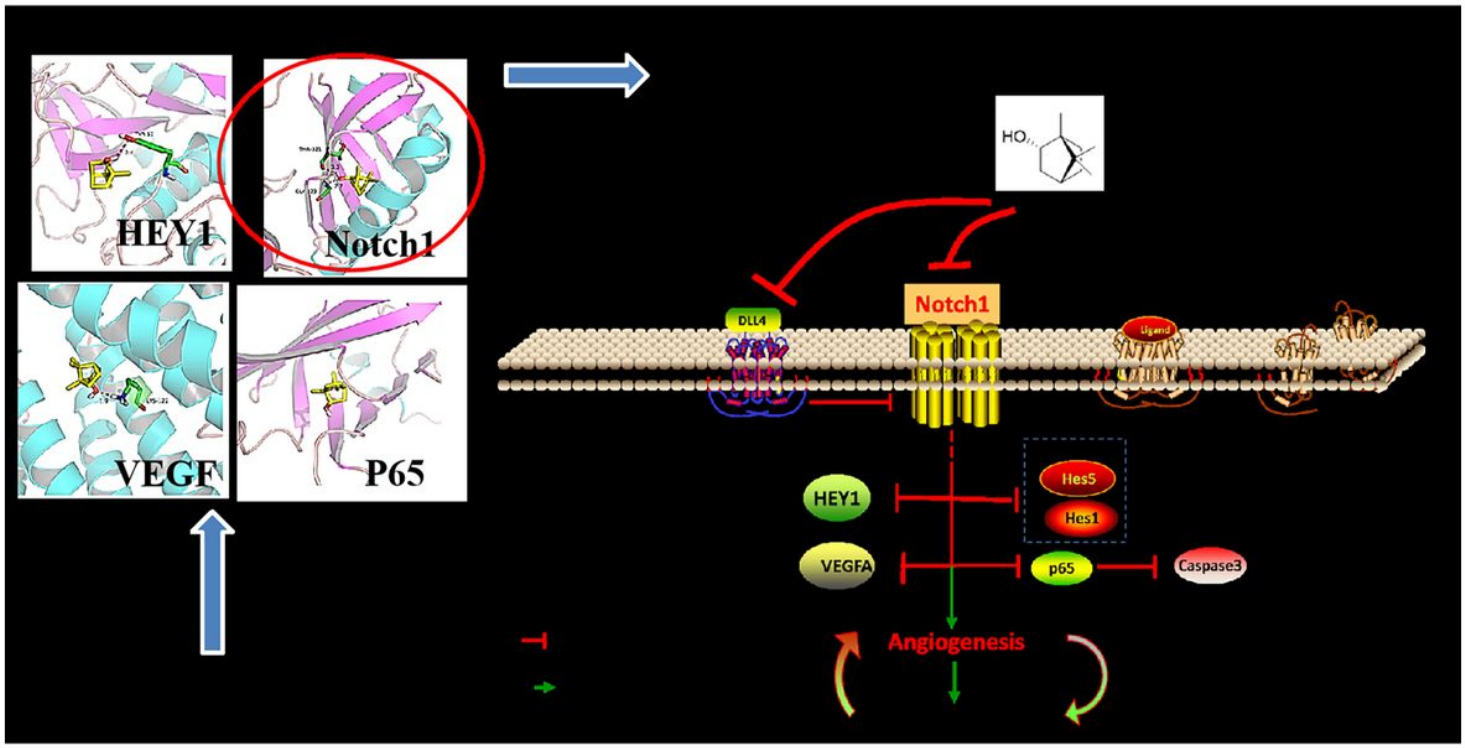

Figure 1

The research scheme and workflow of this study.

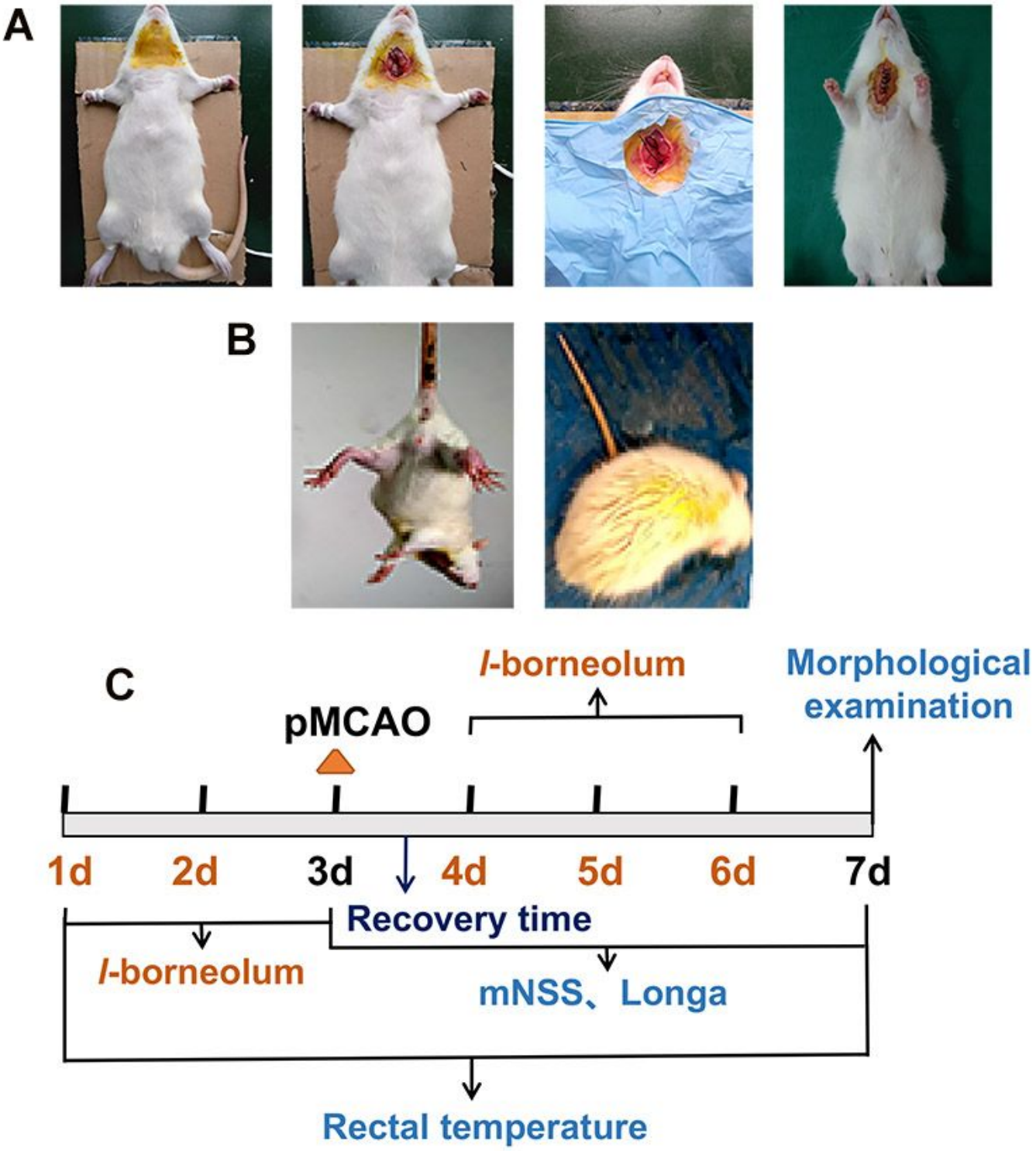

Figure 2

Process of CIS model establishment and the successful status s of pMCAO model rats. (A) Modeling process of CIS in rats. (B) The successful status of pMCAO model rats.

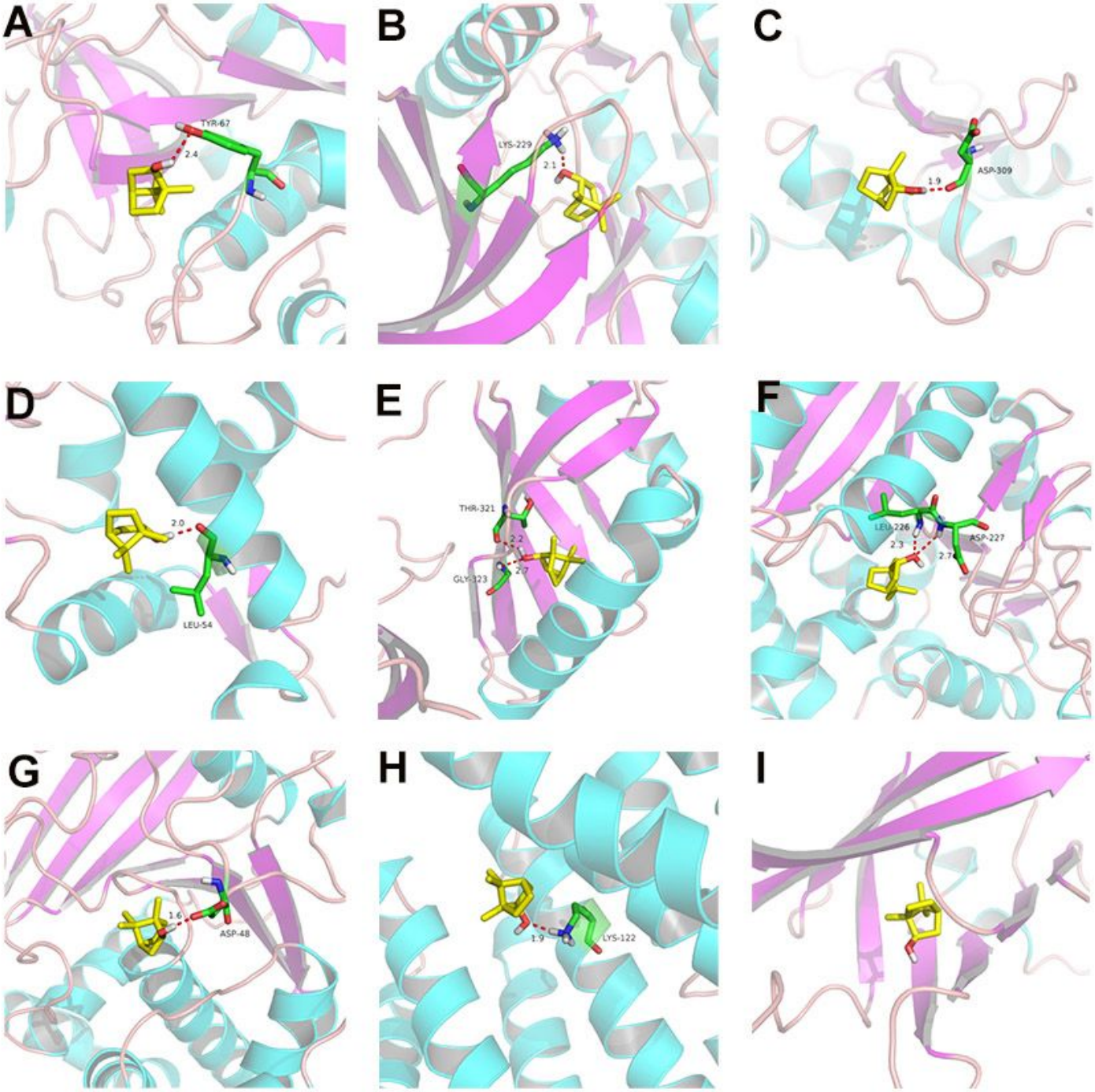

Figure 3

Docking conformation of l-borneolum ligand and related protein. Docking conformation of l-borneolum and CATK protein (A), Hey1 (B), Notch2 (C), p53 protein (D), HIF-1α (E), Notch1 (F), STAT3 (G), p65 (H), VEGFA (I).

Figure 4

Effects of l-borneolum on recovery time and rectal temperature of CIS rats. (A) Effect of l-borneolum on the recovery time of rats after CIS. (B) The change trend graph of the effect of l-borneolum on rectal temperature of rats. (C) The effect of l-borneolum on the rectal temperature of CIS rats before and after administration (Δt1). (D) The effect of l-borneolum on the rectal temperature of CIS rats before and after modeling (Δt2). (E) The effect of l-borneolum on the rectal temperature of CIS rats before and after drug withdrawal (Δt3). Data were expressed as mean ± SD. *p< 0.05 and **p< 0.01 versus the sham group. #p< 0.05 and ##p< 0.01 versus the model group. &p< 0.05 and &&p< 0.01 versus the vehicle group. (n = 12).

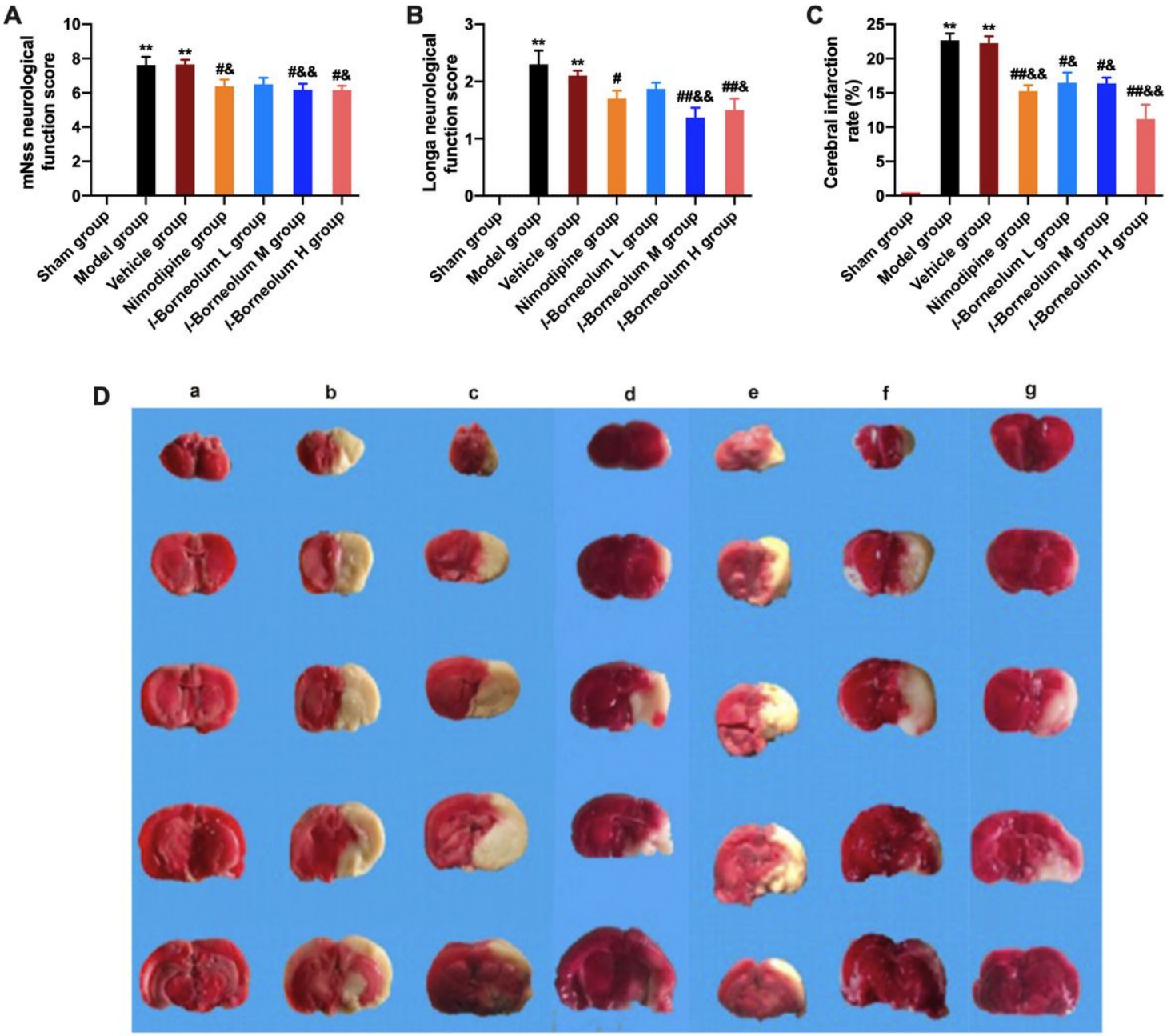

Figure 5

Effects of l-borneolum on neurological function score and cerebral infarction of rats. (A) Effect of l-borneolum on mNss neurological function score of CIS rats (n = 12). (B) Effect of l-borneolum on Longa neurological function score of CIS rats (n = 12). (C) Effect of l-borneolum on cerebral infarction of CIS rats (n = 6). (D) Representative figures for the therapeutic effect of l-borneolum on the morphology of cerebral infarction of CIS rats. Data were expressed as mean ± SD. *p< 0.05 and **p< 0.01 versus the sham group. #p< 0.05 and ##p< 0.01 versus the model group. &p< 0.05 and &&p< 0.01 versus the vehicle group.

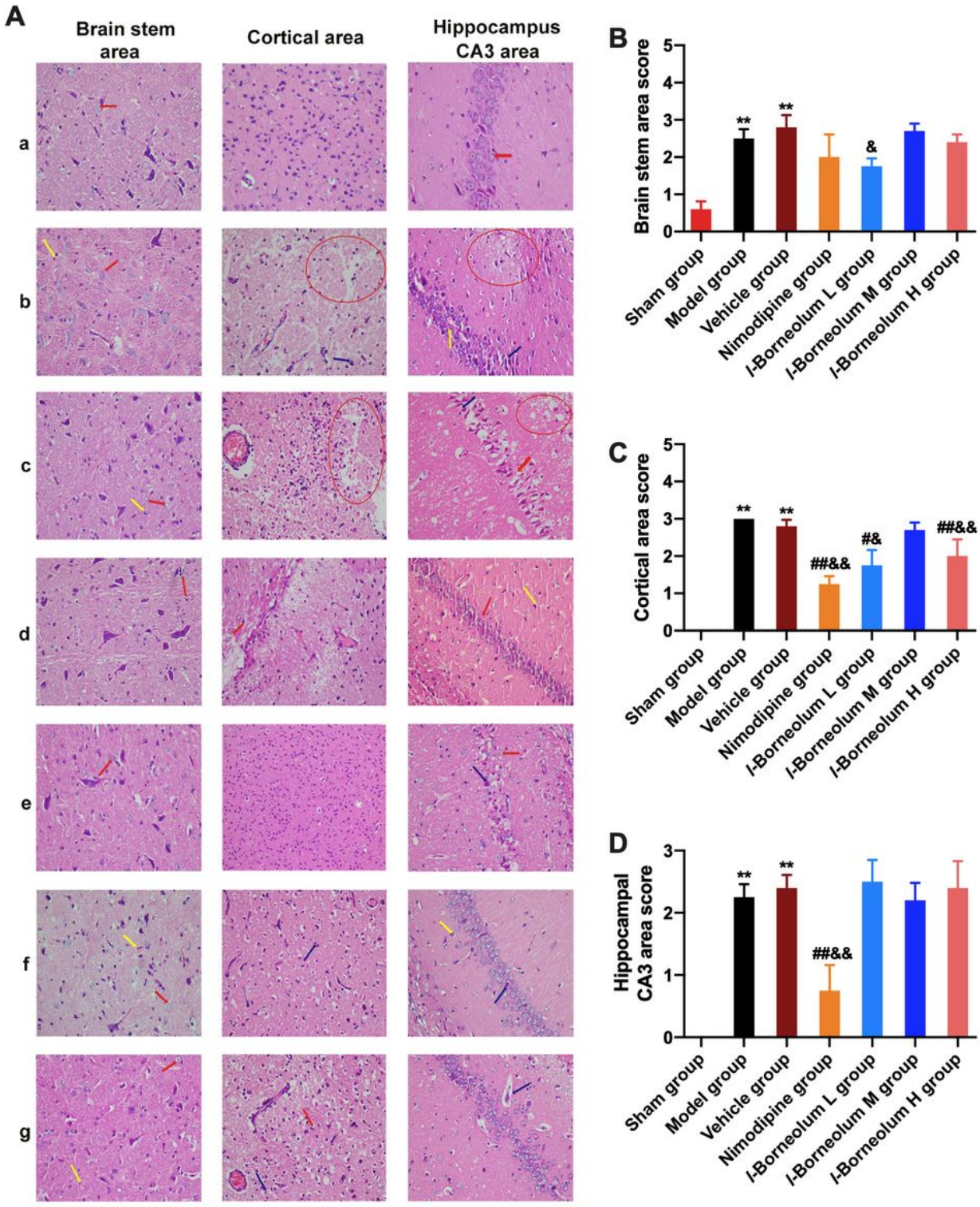

Figure 6

Pathological changes and therapeutic effect of l-borneolum on cerebral tissue. (A) Effects of l-borneolum on pathological changes of CIS rats. (a. sham group; b. model group; c. vehicle group; d. nimodipine group; e. l-borneolum low dose group; f. l-borneolum medium dose group; g. and l-borneolum high dose group). (B) Brain stem area score. (C) Cortical area score.(D) Hippocampal area CA3 score. (HE stained, 200 × magnification)

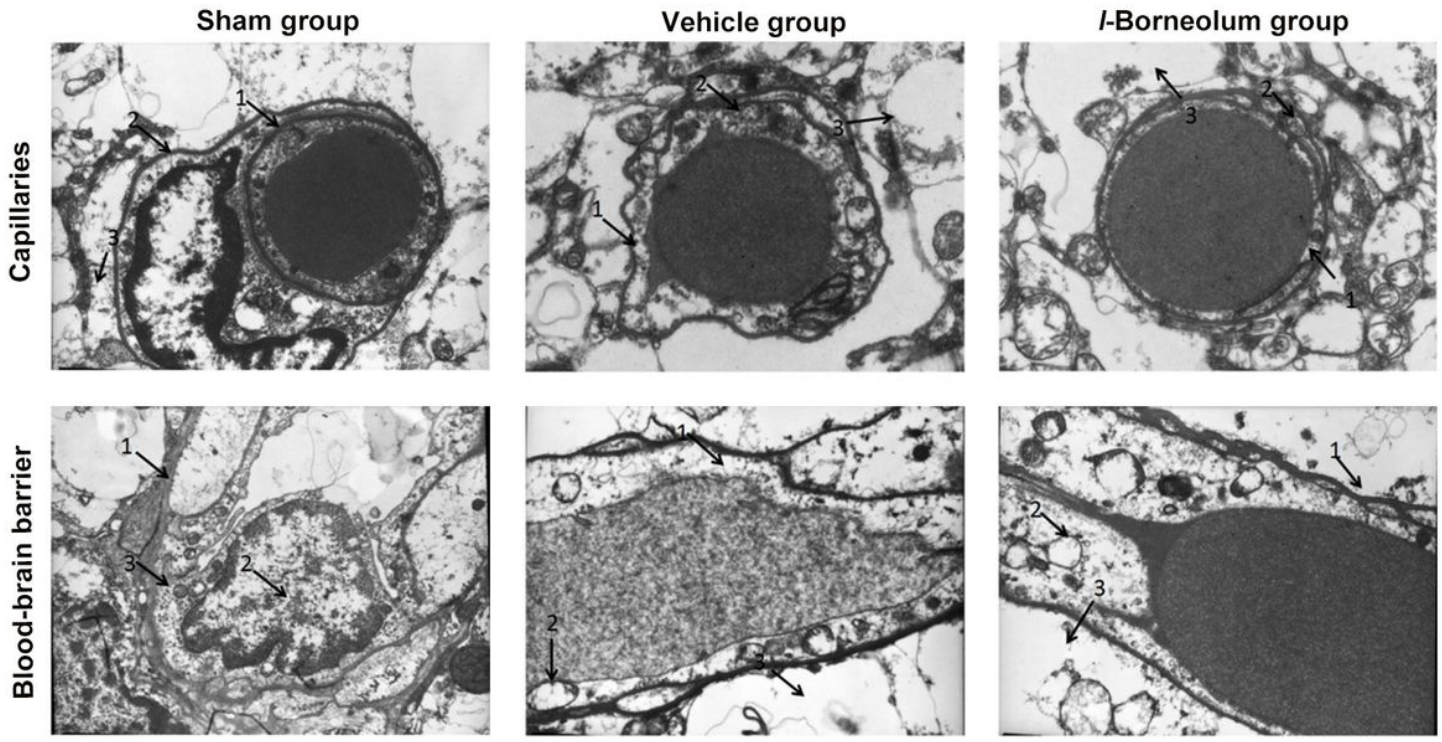

Figure 7

Effect of l-borneolum on ultrastructure of cortical capillaries and blood-brain barrier in CIS rats. (8000 × magnification)

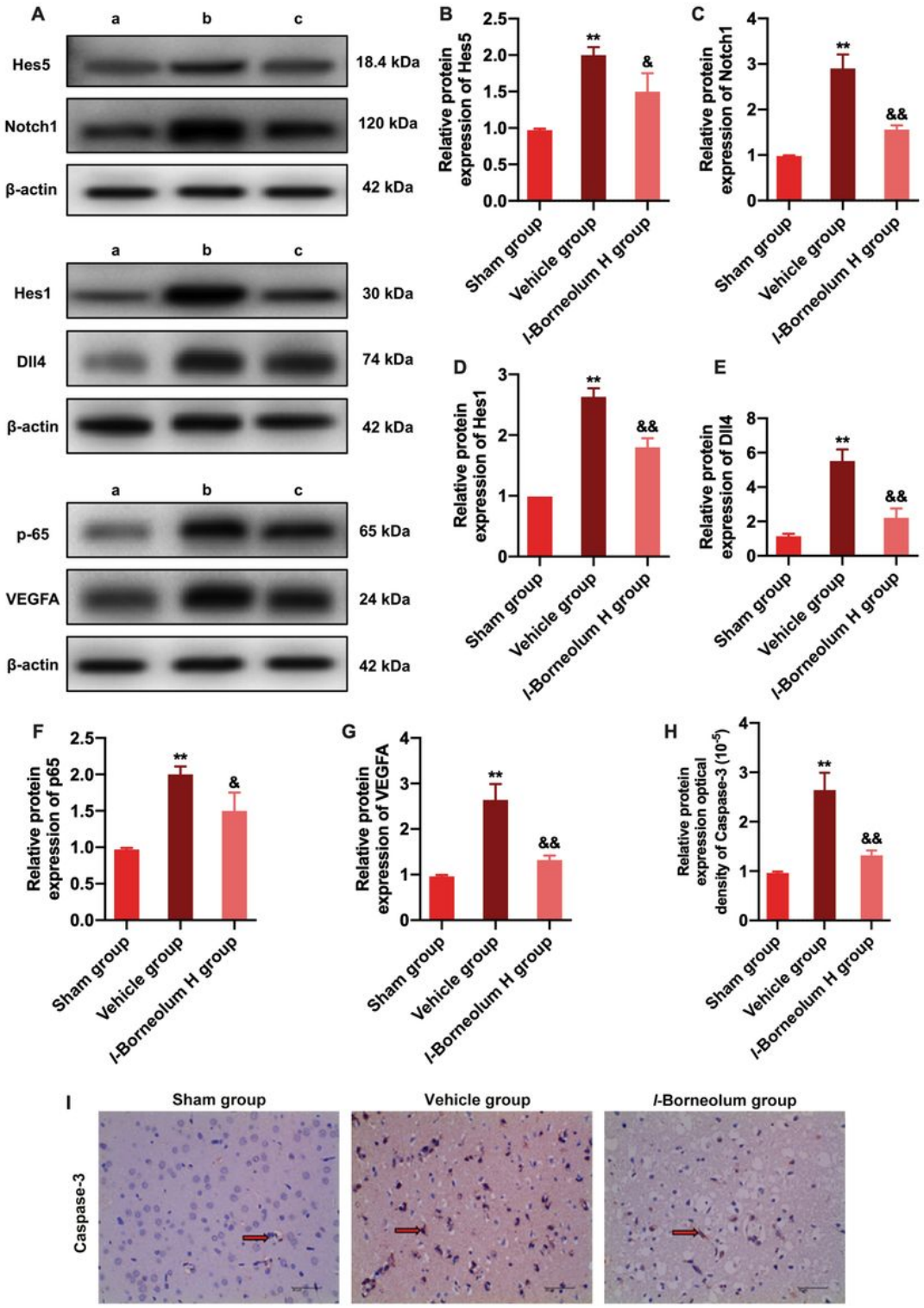

Figure 8

Effects of l-borneolum on the relative protein expression of Notch1 signaling pathway. (A) Western blotting images of Hes5, Notch1, Hes1, Dll4, p-65, and VEGFA in the cerebral cortex of CIS rats. (B) The relative protein expression of Hes5. (C) The relative protein expression of Notch1. (D) The relative protein expression of Hes1. (E) The relative protein expression of Dll4. (F) The relative protein expression of p-65. (G) The relative protein expression of VEGFA. (H) The relative protein expression optical density of

Caspase-3. (I) The level of Caspase-3 in the cerebral cortex of CIS rats was measured using immunohistochemical staining (400 ×). Data were expressed as mean ± SD. *p < 0.05 and **p< 0.01 versus the sham group. #p < 0.05 and ##p < 0.01 versus the model group. &p< 0.05 and &&p < 0.01 versus the vehicle group. (n = 3).

Figure 9

The role of l-borneolum on the Notch signaling pathway. The Notch signaling pathway regulating brain injury after CIS.